23rd ABCM International Congress of Mechanical Engineering
December 6-11, 2015, Rio de Janeiro, RJ, Brazil

A LINEAR STABILITY ANALYSIS OF INCOMPRESSIBLE COAXIAL JETS USING AN ACCURATE BOUNDARY-LAYER APPROXIMATION AS BASE FLOW

Helio Ricardo de Aguiar Quintanilha Junior
Leonardo Santos de Brito Alves
Laboratório de Mecânica Teórica e Aplicada, Departamento de Engenharia Mecânica, Universidade Federal Fluminense, Niterói, RJ, 24210-240, Brazil
helioricardo@id.uff.br, leonardo.alves@mec.uff.br

Oberdan Miguel Rodrigues de Souza
Pontificia Universidade Católica do Rio de Janeiro, Rio de Janeiro, RJ, 22451-900, Brazil
oberdanmiguel@gmail.com

Marcio Teixeira de Mendonca
Comando Geral de Tecnologia Aeroespacial, Instituto de Aeronautica e Espaço, São Jose dos Campos, SP, 12228-904, Brazil
marcio-tm@yahoo.com

Abstract. *A linear stability analysis is employed to study convectively unstable incompressible coaxial jets with a momentum thickness that is much smaller than the jet diameter. In other words, curvature effects are neglected and the coaxial jet is modeled as multiple planar mixing-layers. The main goal is to investigate the formation of new modes of instability through the interaction between these mixing-layers. In order to do so, an accurate base flow must be employed. It is created in the present paper by combining individual mixing-layers using matched asymptotic expansions, which generates a solution with the same accuracy order of the standard boundary-layer approximation. Two cases are considered, where the inner nozzle wall separating both streams has negligible as well as non-negligible thickness. Furthermore, two different techniques are used to solve the linear stability problem. First, a matrix forming approach built with second-order finite-differences on non-uniform meshes generates low accuracy estimates for all eigenvalues. Second, these values are used as initial guesses for a shooting method to generate high accuracy solutions for the unstable eigenvalues. Preliminary results obtained so far indicate the appearance of more modes than inflection points for certain parameter choices for both cases considered.*

Keywords: *mixing-layers, double mixing-layer, triple mixing-layer, linear stability analysis, coaxial jets*

1. INTRODUCTION

Generally, aerospace propulsion is achieved by converting internal energy in kinetic energy inside a combustion chamber, generating the necessary impulse. The chemical reactions responsible for this energy are strongly dependent of the mixing process. Therefore, it is very important to understand how the injection system introduces and mixes the fuel with the oxidant inside the combustion chamber. Usually, kerosene, hydrogen and hydrazine are chosen as fuels and oxygen, hydrogen peroxide and di-tetroxide nitrogen as oxidants. The present paper focuses on injection systems used in liquid rocket engines, or LREs. One of the most common and largely utilized is the coaxial shear injector. In this injector, the inner jet contains oxidant and the outer annular jet contains fuel. They can be found in the J-2 engine used in the Saturn V rocket, in the RS-24 engine, also know as the main engine present in the Spatial Station, and the Vulcan engine present in the Ariane 5 rocket. Free jets, individual or coaxial, are highly unstable shear flows, making their mixing capability highly susceptible to flow excitation. They can be produced from several sources, such as structural vibration, wall roughness and so on. One of the main goals of the injection system designers is to avoid resonance between the jet generated noise and the combustion chamber acoustics, which can drastically modify the mixing characteristics of the jet. As a direct consequence, combustion can happen far away from its designed conditions, causing severe damage to the engine and even destruction of the entire vehicle.

2. LINEAR STABILITY ANALYSIS

Instability is the inability of a given pattern in a physical system to be maintained once subject to small disturbances (Chandrasekhar, 1961). Such disturbances can appear due to various factors such as structure vibrations, noise, turbulence, roughness, among others. The analysis attempts to determine the response of a steady state to small disturbances. If the disturbance amplitude decreases, the system is stable to that particular disturbance. If its amplitude increases so that the perturbed system diverts from its original state, the system is said to be unstable. According Salemi (2006), the theory of hydrodynamic stability investigates how disturbances in a flow are amplified or damped and how the evolution of these disturbances is related to the transition to turbulent flow phenomenon.

Traditionally, the instability of flows to small amplitude perturbations has been analysed using the modal approach (Juniper *et al.*, 2013). Given an operator that describes the evolution of small perturbations, this approach considers the temporal or spatial development of individual eigenmodes of that operator. The resulting linear stability theory (LST) relies on the decomposition of any flow quantity $\mathbf{q}$ into a steady part $\overline{q}$, which is usually called the base flow, and an unsteady part $\tilde{q}$

$$\mathbf{q}(\mathbf{s},t) = \overline{\mathbf{q}}(\mathbf{s}) + \varepsilon\tilde{\mathbf{q}}(\mathbf{s},t) \tag{1}$$

where $\mathbf{s}$ is the space coordinate vector, given by (x,y,z), t is time e $\varepsilon \ll 1$ is a small amplitude.

Explicitly, the perturbation vector $\tilde{\mathbf{q}}$ present in the Eq.1 takes the form of:

$$\tilde{\mathbf{q}} = \hat{\mathbf{q}}e^{i\Theta} \tag{2}$$

where $\hat{\mathbf{q}}$ and Θ are the amplitude and phase functions of the linear perturbations, respectively. According to the literature (Lin, 1955; Drazin, 1969; Mack, 1984)), the base flow is considered homogeneous over two spatial directions, which is known as the parallel flow assumption. In this case, the derivative of the flow in these directions is negligible. Furthermore, the velocity component normal to the wall is assumed negligible for incompressible flows. Hence, for the two dimensional case:

$$\tilde{\mathbf{q}}(x,y,t) = \hat{\mathbf{q}}(y)e^{i(\alpha x - \omega t)} \tag{3}$$

which is used in this paper. More details about this derivation are given elsewhere (Juniper *et al.*, 2013).

2.1 Spatial Stability Analysis

Generally, ω and α from equation 3 can be complex numbers. However, in order to do a spatial analysis, we can assume a constant real monochromatic frequency ω. The wave-number α in equation 3 remains complex and is an eigenvalue of the problem. From this point of view, the linear perturbations can be written as:

$$\tilde{\mathbf{q}} = \hat{\mathbf{q}}(y)e^{i[(\alpha_r + i\alpha_i)x - \omega t]} \tag{4}$$

where $-\alpha_i$ is the spatial amplification rate of the wave and α_r its wave-number. From a theoretical/numerical point of view, the eigenvalue problem to be solved is non-linear for viscous flows (Juniper *et al.*, 2013).

It is also necessary to distinguish three types of instability, according to their response to an impulse disturbance. The flow is said to be stable if the impulse response decays in every direction. A flow is convectively unstable if the impulse response grows along some rays that move away from the point of impulse but decays at the point of impulse itself. A flow is absolutely unstable if the impulse response grows at the point of impulse. For an elaboration on that idea, a reading of Huerre and Monkewitz (1990) becomes essential. More details can be found in the works of Huerre and Rossi (1998) and Huerre *et al.* (2000).

In the case of a mixing layer, a spatial stability analysis can be performed because the flow becomes convectively unstable for positive Reynolds numbers. As mentioned by Monkewitz and Huerre (1982), the results of spatial analysis agree very well with experimental data.

3. BASE FLOW

3.1 Similarity

Several approaches can be used for the construction of the base flow. Boundary layer theory is used here to build the base flow, but some conditions must be satisfied. In general, flow variables in a two-dimensional boundary layer depend on both spatial coordinates. Thus, different velocity profiles are found at different downstream locations. However, a similarity transformation can be used to reduce the number of independent variables to η, i.e., all downstream velocity profiles collapse into a single curve. The region of the mixing layer that behaves this way is known as similar region and its solutions are known as similar solutions (Salemi, 2006).

It is important to say that the downstream location chosen is of great importance for a valid similar solution. A location too close to the splitter plate includes wake effects not present in a boundary-layer model whereas a location too far from this point goes into the transition / turbulent region. Therefore, the point chosen for the calculation should be far enough so the profiles become similar, but not so far in order to leave the laminar flow region.

4. MIXING-LAYER: LINEAR STABILITY ANALYSIS

The mixing layer is the region of interaction between fluids, initially separated by a splitter plate that keeps them parallel until its end, where the fluids meet forming an interface. This interface is defined by the maximum gradient region between these layers. Small perturbations grow and lead to the emergence of transverse vortexes, the beginning of a process that eventually leads to a turbulent regime. A mixing layer may be classified according to the number of inflection points within it.

4.1 Double Mixing Layer

Beyond the classical single mixing layer, multiple mixing layers will be considered next. Since the thickness of the jet mixing layer is much smaller than the jet diameter, the curvature effects can be neglected and the coaxial jet can be modelled as multiple planar mixing-layers. Therefore, a double mixing layer contains two interfaces separating three flows. In the double layer, there is no separation region between the flows, so that they interact with each other immediately after the nozzle outlet. In other words, the nozzle wall has a negligible thickness.

4.2 Triple Mixing Layer

For the stability analysis of a triple mixing layer, a separation region due to a nozzle wall of finite thickness is considered. The application of this thickness causes a viscous wake region to emerge from the mixing layer. This feature possibly induces a transition from convective to absolute instability as well as creates new unstable modes. In this case, tree interfaces separate four flows.

5. OBJECTIVES

The purpose of this paper is to investigate the hydrodynamic instability in coaxial incompressible jets through the linear stability analysis technique. In order to do so, three key things are pursued:

1) The construction of the steady base profile using similarity solutions for double and triple mixing layers;

2) The modes of instability found due to interaction between double and triple layers;

3) The pursuit of transitional instability due to interaction between the layers.

6. MATHEMATICAL FORMULATION

6.1 Linearized Navier Stokes Equation

Substituting equation 1 into the Navier-Stokes equations, subtracting the equations for the base flow, and dropping the terms of order ϵ^2 yields the linearized perturbation equations, referred to as the linearized Navier-Stokes equations - **LNSE** and continuity equation. In an incompressible flow, they are

$$\frac{\partial \tilde{\mathbf{u}}}{\partial t} + \tilde{\mathbf{u}}.\nabla\mathbf{U} + \mathbf{U}.\nabla\tilde{\mathbf{u}} = -\nabla\tilde{p} + \frac{1}{Re}\nabla^2\tilde{\mathbf{u}} \qquad \nabla\tilde{\mathbf{u}} = 0 \qquad Re = \frac{\mathbf{U}\delta_0}{\nu} \tag{5}$$

where U is the base flow and $\tilde{u}$ is the perturbation.

By introducing the basic state defined by normal modes from the equation 2, **LNSE** turns into an eigenvalue problem. Defining the spatial coordinates as (x,y) for the two dimensional case we have the following equations:

$$i\alpha\hat{u} + \frac{\partial\hat{v}}{\partial y} = 0 \qquad i\alpha(U-c)\hat{u} + \frac{\partial U}{\partial y}\hat{v} + i\alpha\hat{p} = \frac{1}{Re}(\frac{\partial^2\hat{u}}{\partial y^2} - \alpha^2\hat{u}) \qquad i\alpha(U-c)\hat{v} + \frac{\partial\hat{p}}{\partial y} = \frac{1}{Re}(\frac{\partial^2\hat{v}}{\partial y^2} - \alpha^2\hat{v}) \tag{6}$$

where c is the phase speed defined as ω/α.

6.2 The Orr-Sommerfeld Equation

Equation 6 can be rearranged and written in the form of a single ordinary differential equation of fourth order

$$\frac{i}{Re}[\hat{v}^{(4)} - 2\alpha^2\hat{v}^{''} + \alpha^4\hat{v}] + \alpha(U-c)[\hat{v}^{''} - \alpha^2\hat{v}] - \alpha U^{''}\hat{v} = 0 \tag{7}$$

for the transverse velocity perturbation known as the Orr-Sommerfeld equation.

6.3 The Rayleigh Equation

In the limit $Re \to \infty$, the viscous terms of the Orr-Sommerfeld equation 7 can be dropped, giving rise to:

$$\alpha(U-c)[v^{''}-\alpha^2\hat{v}]-\alpha U^{''}\hat{v}=0 \tag{8}$$

which is the equation used in this paper.

6.4 Boundary Layer Equation

A similar conservation equation for the incompressible laminar boundary layer problem is given by:

$$2f^{'''}+ff^{''}=0 \tag{9}$$

with the following boundary conditions:

$$f(0)=0 \qquad f'(-\infty)=1 \qquad f'(\infty)=VR \tag{10}$$

where VR is the velocity ratio between layers. Thus we have the dimensional velocity and vorticity given by:

$$u^*=U_\infty f' \qquad \frac{du^*}{dy^*}=\frac{U_\infty}{\delta_\infty}f'' \tag{11}$$

7. NUMERICAL METHOD

To study the hydrodynamic stability of the mixing layer we need to solve the laminar base flow through similar equations and then solve the stability equations. From the stability equations arises an eigenvalue problem where we search for the eigenvalue α, which provides the growth ratio of the perturbations. In order to achieve this, it was developed a notebook in the software *MATHEMATICA* and codes in *FORTRAN 90* language.

7.1 Base Flow: Shooting Method

In order to simulate the base flow, the shooting method was chosen. It turns a boundary value problem into an initial value problem. Before using this approach, equation 9, which is a differential equation of order three, is rewritten as a system of three first order equations, as follows:

$$f'=df \qquad df'=ddf \qquad 2ddf'+fdf'=0 \tag{12}$$

which requires three initial conditions

$$f(0)=0 \qquad df(0)=cte1 \qquad ddf(0)=cte2 \tag{13}$$

where the constants will be estimated together with the eigenvalues. This system is integrated towards the already known boundary conditions at $+\infty$. In order to do so, the command **NDSolve** present in the Software *Mathematica* was chosen to perform this integration, which has an automatic error control and switchs between more efficient methods according to the problem stiffness. The command **FindRoot** was used to search for the constants and eigenvalues that lead to a solution that satisfies the original boundary conditions $+\infty$. After that, the **NDSolve** command is used again in order to solve the differential equation with the correctly calculated constants and eigenvalues.

7.2 Base Flow: Matched Asymptotic Expansions

After calculating the similarity solution for each boundary layer, we need to construct the multiple boundary layer solution in order to form the necessary base flow for the coaxial jet stability analysis. Matched asymptotic expansions are employed for this purpose because the resulting solution maintains the accuracy order of the individual solutions.

7.2.1 Double Mixing Layer

For the double mixing layer, two boundary layer solutions are required. The first one refers to layers 1 and 2. For the first layer U_1 and U_2 represent the velocity of inner and outer jets, respectively, $\delta_{1,2}$ the momentum thickness between them and $\eta = y/\delta_{1,2}$, then:

$$f'_{1,2}(-\infty)=1 \qquad f'_{1,2}(\infty)=VR_{1,2}=\frac{U_2}{U_1} \tag{14}$$

where dimensional velocity and vorticity profiles are defined as:

$$u^*_{1,2} = U_1 f'_{1,2} \qquad \frac{du^*}{dy^*}|_{1,2} = \frac{U_1}{\delta_{1,2}} f''_{1,2} \tag{15}$$

For the second solution, U_3 is the flow velocity outside the coaxial jet, which is assumed zero, $\delta_{2,3}$ is the momentum thickness between layers 2 and 3 and $\eta = y/\delta_{2,3}$, leading to

$$f'_{2,3}(-\infty) = 1 \qquad f'_{2,3}(\infty) = VR_{2,3} = \frac{U_3}{U_2} \tag{16}$$

where the dimensional velocity and vorticity profiles are:

$$u^*_{2,3} = U_2 f'_{2,3} \qquad \frac{du^*}{dy^*}|_{2,3} = \frac{U_2}{\delta_{2,3}} f''_{2,3} \tag{17}$$

Both profiles can be combined to generate

$$u = \{f'_{1,2}[\frac{y^*}{\delta_{1,2}}]\}_{+\Delta y} + \{VR_{1,2} f'_{2,3}[\frac{y^*}{\delta_{2,3}}]\}_{-\Delta y} - VR_{1,2} \tag{18}$$

where δ_R can be introduced as a characteristic thickness to write $y = y^*/\delta R$, leading to velocity profile

$$u = \{f'_{1,2}[\frac{\delta_R}{\delta_{1,2}} y]\}_{y \to y+\Delta y} + \{VR_{1,2} f'_{2,3}[\frac{\delta_R}{\delta_{2,3}} y]\}_{y \to y-\Delta y} - VR_{1,2} \tag{19}$$

and vorticity profile

$$\frac{du}{dy} = \{\frac{\delta_R}{\delta_{1,2}} f''_{1,2}[\frac{y^*}{\delta_{1,2}}]\}_{+\Delta y} + \{VR_{1,2} \frac{\delta_R}{\delta_{2,3}} f''_{2,3}[\frac{y^*}{\delta_{2,3}}]\}_{-\Delta y} - 0 \tag{20}$$

Introducing $\Delta_{1,3}$ as the distance between infection points, one can write the double mixing layer profiles as

$$u = f'_{1,2}[\frac{\delta_R}{\delta_{1,2}}(y + \frac{\Delta_{1,3}}{2})] + VR_{1,2} f'_{2,3}[\frac{\delta_R}{\delta_{2,3}}(y - \frac{\Delta_{1,3}}{2})] - VR_{1,2} \tag{21}$$

and

$$\frac{du}{dy} = \frac{\delta_R}{\delta_{1,2}} f''_{1,2}[\frac{\delta_R}{\delta_{1,2}}(y + \frac{\Delta_{1,3}}{2})] + VR_{1,2} \frac{\delta_R}{\delta_{2,3}} f''_{2,3}[\frac{\delta_R}{\delta_{2,3}}(y - \frac{\Delta_{1,3}}{2})] \tag{22}$$

for velocity and vorticity. The triple mixing layer is constructed in a similar way.

7.3 Stability Analysis: Shooting Method

As noted earlier for a spatial stability analysis, the eigenvalue sought is α, which is complex, and the frequency ω, which is real. When using the shooting method to solve the Rayleigh equation, a real frequency is fixed and an initial guess is assumed for the wave-number. This equation is numerically integrated from both sides of the far field towards the centre of the domain, where velocity continuity is verified using a Wronskian. If it is not satisfied, a new value is assigned to the wave-number in a process that is repeated until continuity is satisfied.

7.3.1 Dispersion Relation

The problem then comes down to finding an initial estimate for the wave-number that approximately satisfies the dispersion relation $f(\alpha, \omega) = 0$. In order to do so, a mesh is created for the real and imaginary parts of α. A contour plot of the interpolated zero real and imaginary parts of the dispersion relation is made, for a fixed frequency. The point of intersection between these two curves is the graphical estimate for the complex wave-number. As the frequency is increased, extrapolation is employed to generate new estimates for the wave-number.

7.4 Stability Analysis: Matrix Forming

When using the matrix forming method, equations 6 are discretized using second order finite differences, leading to an algebraic system of equations in the form of

$$A\overline{q} = \alpha B\overline{q} + \alpha^2 C\overline{q} \tag{23}$$

which is nonlinear for the wave number α. However, by creating the new variable ser $\alpha q = \overline{q}$, it is possible to write a lienar version of the same problem in the form of

$$\overline{A}\overline{q} = \alpha\overline{B}\overline{q} \tag{24}$$

where the well known QZ algorithm is here used. Although the system in 24 is larger than its counterpart 23, it is now possible to generate the full spectrum of wave numbers.

8. RESULTS

8.1 Double Mixing Layer

8.1.1 Base Flow

Figure 1 illustrates the double mixing layer parameters used in the present analysis. They are defined as the velocity ratio between the layers, $VR_{1,2}$, the momentum thickness between the layers, $\delta_{1,2}$ and $\delta_{2,3}$, and the distance between coaxial jet inflection points, $\Delta_{1,3}$. The values studied here are given in Table 1.

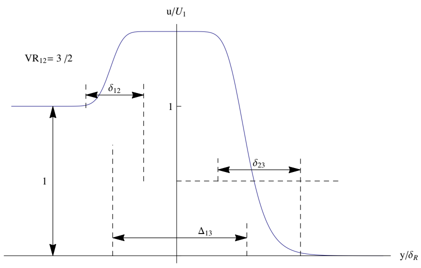

Figure 1. Base Flow for Double Mixing Layer

Table 1. Variation of different parameters analysed in a double mixing layer.

VR	$\Delta y/\delta R$	$\delta_{1,2}$	$\delta_{2,3}$
3/2	8	1/60, 1/40, 1/20 and 1/10	1/40
3/2	8	1/40	1/60, 1/40, 1/20 and 1/10
3/2	8, 6, 4, 3, 2 and 1	1/40	1/40

8.1.2 Linear Stability Analysis

In the first analysis, the thickness of the inner layer $\delta_{1,2}$ is varied to yield the results in Fig. 2. It was possible to notice that for each case, two modes were presents, as expected for the double mixing layer. It is also relevant to consider that varying the inner layer thickness affects only the second mode. When the thickness decreases, the second mode growth rate increases in magnitude and the range of unstable frequencies also increases.

A similar behaviour is observed when varying the thickness of the outer layer $\delta_{2,3}$ in Fig. 3. The first mode growth rate increases, as does its range of unstable frequencies, as this thickness decreases. Therefore, the first mode is associated with the outer jet and the second mode is associated with the inner jet. This is expected due to the vorticity difference between both jets, since this is the most important parameter controlling growth rate magnitude.

Finally, the range of unstable frequencies does not change when the distance between inflection points is decreased, as shown in Fig. 4. However, the second mode growth rate decreases continually to zero. At the same time, the first mode asymptotes towards the single mixing layer mode.

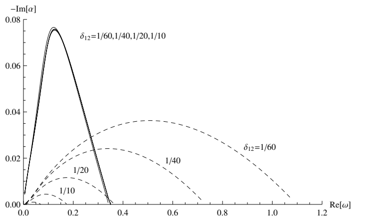

Figure 2. Growth rate vs frequency with VR = 3/2, Δ_{13}/δ_R = 8 and $\delta_{2,3}$ = 1/40

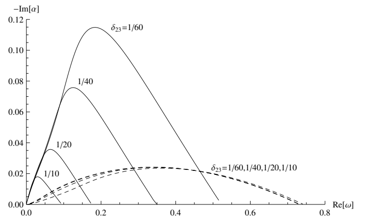

Figure 3. Growth rate vs frequency with VR = 3/2, Δ_{13}/δ_R = 8 and $\delta_{1,2}$ = 1/40

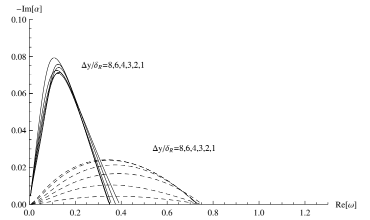

Figure 4. Growth rate vs frequency with VR = 3/2, Δ_{13}/δ_R = 8 and $\delta_{1,2}$ = 1/40

8.2 Triple Mixing Layer

8.2.1 Base Flow

Figure 5 illustrates the triple mixing layer parameters used in the present analysis. The additional parameters are defined as the velocity ratio between the second and third layers, $VR_{2,3}$, and the distances between coaxial jet inflection points, $\Delta_{1,2}$ and $\Delta_{2,3}$. It is important to note that the momentum thickness on both sides of the outer jet, $\delta_{2,3}$, is assumed equal. The values studied here are given in Table 2.

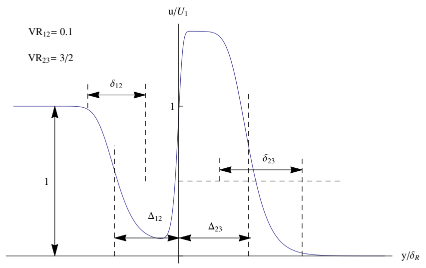

Figure 5. Base Flow for Triple Mixing Layer

Table 2. Variation of different parameters analysed in a triple mixing layer.

VR1	VR2	$\Delta_{1,2}/\delta R$	$\Delta_{2,3}/\delta R$	$\delta_{1,2}$	$\delta_{2,3}$	δ_R
3/2	0.1	8	8, 6, 4, 2 and 1	1/40	1/40	1/40
5	0.1	20	30	1/40	1/40	1/40
5	0.1	25	30	1/40	1/40	1/40
5	0.1	30	30	1/40	1/40	1/40
5	0.1	35	30	1/40	1/40	1/40

8.2.2 Linear Stability Analysis

Triple mixing layers results present three different unstable modes, which are shown separately in Figs. 6 and 7 to avoid the curve overlapping that would occur if presenting all results in the same figure. Furthermore, the first mode, shown in Fig. 6, is three to four times higher than the other two modes, shown in Fig. 7.

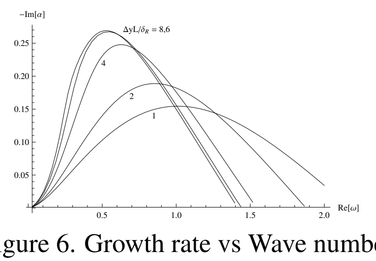

Figure 6. Growth rate vs Wave number

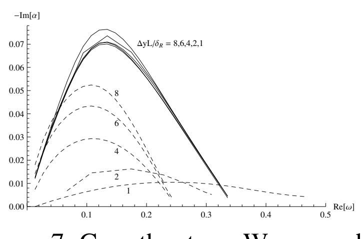

Figure 7. Growth rate vs Wave number

Here, tree modes where found, normally expected by the triple layer. It is also important to say that only the first and third modes were effect by decreasing the outer jet size. Following the example of the double mixing layer, decreasing the outer jet size, decreases also the modes.

In the next cases, the influence of the size of the wall between the jets will be analysed. In this cases the outer jet velocity is much faster as the inner jet and the size of the outer jet is maintained constant as showed in table 2.

However, when the size of the wall increases, a "pinching point" is suppose to appear, as seeing in the literature (Koch, 1985). That point indicate a transition of convectively to absolute instability, where the perturbation start to grow not only downstream but also upstream. This "pinching point" can best be seen in a Growth rate x Wave number graphic. As far as the wall size changes, the probability to a interaction between the stable and the unstable modes increases.

For the cases set in table 2, the results are:

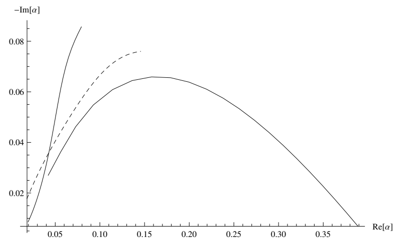

Figure 8. Growth rate vs Wave number with $\Delta_{1,2}/\delta R = 20$

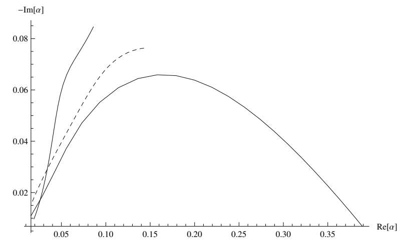

Figure 9. Growth rate vs Wave number with $\Delta_{1,2}/\delta R = 25$

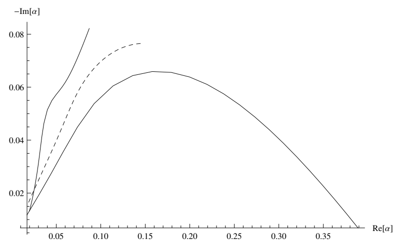

Figure 10. Growth rate vs Wave number with $\Delta_{1,2}/\delta R = 30$

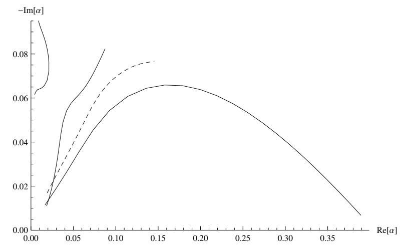

Figure 11. Growth rate vs Wave number with $\Delta_{1,2}/\delta R = 35$

In the cases above, it is possible to see that, by increasing the wall size, nothing much happens with the first mode, but the others are changing. In the last case Fig. 11, where a mode that is stable is showed, it can see that he is beginning to interact with the unstable mode, making the unstable mode change his appearance. When these curves join with each other is when and where the "pinching point" is found and hence, a transition of instability.

9. REFERENCES

Chandrasekhar, S., 1961. "Hydromagnetic and hydrodynamic stability". *Clarendon, Oxford*.

Drazin, P., 1969. "G. & reid, wh 1981 hydrodynamic stability". *Cambridge University Press*, Vol. 2, No. 79, pp. 267–269.

Huerre, P. and Rossi, M., 1998. "Hydrodynamic instabilities in open flows". *COLLECTION ALEA SACLAY MONOGRAPHS AND TEXTS IN STATISTICAL PHYSICS*, pp. 81–294.

Huerre, P., Batchelor, G., Moffatt, H. and Worster, M., 2000. "Open shear flow instabilities". *Perspectives in Fluid Dynamics*, pp. 159–229.

Huerre, P. and Monkewitz, P.A., 1990. "Local and global instabilities in spatially developing flows". *Annual review of fluid mechanics*, Vol. 22, No. 1, pp. 473–537.

Juniper, M.P., Hanifi, A. and Theofilis, V., 2013. "Modal stability theory".

Koch, W., 1985. "Local instability characteristics and frequency determination of self-excited wake flows". *Journal of Sound and Vibration*, Vol. 99, No. 1, pp. 53–83.

Lin, C.C., 1955. "The theory of hydrodynamic stability".

Mack, L.M., 1984. "Boundary-layer linear stability theory". Technical report, DTIC Document.

Monkewitz, P.A. and Huerre, P., 1982. "Influence of the velocity ratio on the spatial instability of mixing layers". *Physics of Fluids (1958-1988)*, Vol. 25, No. 7, pp. 1137–1143.

Salemi, L., 2006. *ANÁLISE DE ESTABILIDADE LINEAR DE CAMADA DE MISTURA COMPRESSÍVEL BINÁRIA*. Master's thesis.

10. RESPONSIBILITY NOTICE

The authors are the only responsible for the printed material included in this paper.